



FULLY MESH-FREE LAGRANGIAN SIMULATIONS USING SPH METHOD

L. Lobovský*, J. Křen*

Summary: *The study is focused on the advantages of numerical simulations based on the meshless Lagrangian approach to continuum description. The formulation of the smoothed particle hydrodynamics (SPH) method and its implementation for problems of incompressible fluid dynamics is presented. The results of numerical simulations of problems involving free surfaces and fluid to fluid interaction are displayed.*

1. Introduction

The smoothed particle hydrodynamics (SPH) is a meshless numerical method utilising the Lagrangian approach to continuum description. In general, the Lagrangian description is advantageous for the problems featuring a complex geometry of the computational domain, while the meshless representation of the continuum is convenient especially within simulations of materials undergoing large deformations. The first papers on the SPH method were published by Gingold & Monaghan (1977) and Lucy (1977). Originally, the SPH method was applied within gas dynamics problems in astrophysics, but during last three decades, the SPH method as one of the oldest meshless approaches spread into numerous branches of computational physics. The general review of the SPH method development can be found in e.g. Vignjevic (2004), Liu & Liu (2003), Monaghan (1992). This paper concerns about the SPH application within problems of the incompressible fluid dynamics involving free surfaces and fluid to fluid interaction. It compiles the knowledge gained from the previously published studies on the incompressible viscous flow modelling, Morris et al. (1997), free surface flow simulations, Monaghan (1994), Liu & Liu (2003) and multi-phase flows, Monaghan & Kocharyan (1995), Colagrossi & Landrini (2003).

2. SPH Formulation

Within the SPH formulation, the computational grid is replaced by a finite set of interpolating points. The interpolating points are called particles and their coordinates are invariant in the material frame. They represent a finite mass of the discretised continuum and carry the information about all physical variables which are evaluated at their positions. Within a certain range of applications, the SPH particles may also be applied to model the real material particles, but only the SPH representation of continuous material is considered within this study. The function value f_i at a specific particle at the position \mathbf{r}_i is interpolated from the

* Ing. Libor Lobovský, Prof. Ing. Jiří Křen, CSc.: Department of Mechanics, University of West Bohemia in Pilsen; Univerzitní 22; 30614 Plzeň; tel.: +420 377 632 336, fax: +420 377 632 302; e-mail: lobo@kme.zcu.cz

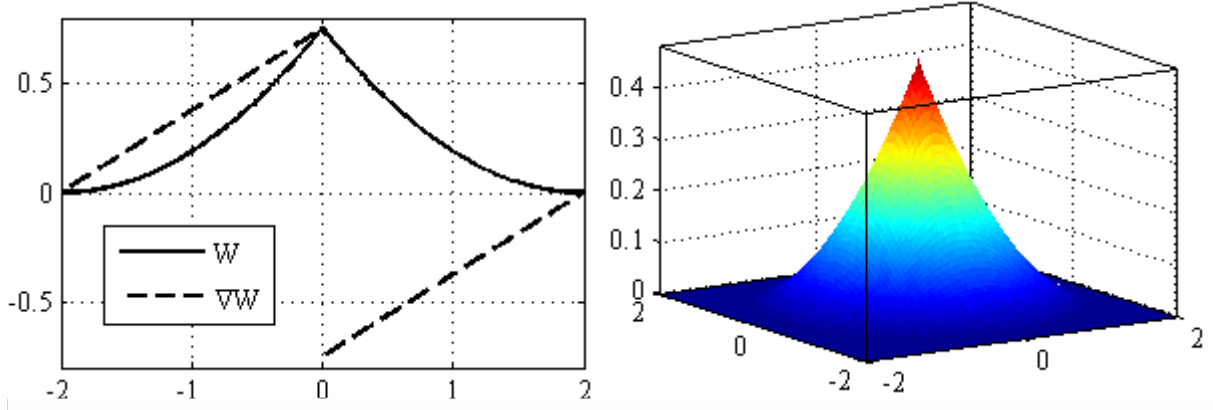


Fig. 1. The quadratic smoothing function W and its first derivative in 1D (left), the quadratic smoothing function W in 2D (right).

function values f_j at surrounding particle positions \mathbf{r}_j . The general SPH equations may be derived as (see e.g. Monaghan (1992) for details)

$$f_i = \sum_j \frac{m_j}{\rho_j} f_j W(|\mathbf{r}_i - \mathbf{r}_j|, h), \quad (1)$$

$$\nabla_i f_i = \sum_j \frac{m_j}{\rho_j} f_j \nabla_i W(|\mathbf{r}_i - \mathbf{r}_j|, h), \quad (2)$$

where m is the mass, ρ is the density and W is the interpolating (smoothing) function with a continuous derivative $\nabla_i W$. The subscripts i, j denotes the variables at the particle i, j , respectively, and ∇_i denotes a derivative according to \mathbf{r}_i . The smoothing function depends on the distance between the pair of interacting particles and the smoothing length h and is defined according to the conditions (3) and (4),

$$W(|\mathbf{r}_i - \mathbf{r}_j|, h) = 0 \quad \text{for } |\mathbf{r}_i - \mathbf{r}_j| \geq \lambda h, \quad (3)$$

$$\int_{\Omega} W(|\mathbf{r}_i - \mathbf{r}_j|, h) d\mathbf{r}_j = 1. \quad (4)$$

The smoothing function W has a compact support domain defined by a finite multiple of the smoothing length λh , its value monotonously decreases as the distance between particles increases and in the limit case, when the smoothing length h tends to zero, the smoothing function becomes the Dirac delta function. Details on deriving the smoothing functions and a list of various smoothing function definitions are given in Liu & Liu (2003). In order to satisfy the condition (4), the smoothing function has to be normalised respecting the spatial dimension of the solved problem. Within this study, the quadratic smoothing function definition is applied,

$$W(|\mathbf{r}_i - \mathbf{r}_j|, h) = \frac{N}{h^D} \left[\frac{3}{16} \left(\frac{|\mathbf{r}_i - \mathbf{r}_j|}{h} \right)^2 - \frac{3}{4} \left(\frac{|\mathbf{r}_i - \mathbf{r}_j|}{h} \right) + \frac{3}{4} \right], \quad 0 \leq \frac{|\mathbf{r}_i - \mathbf{r}_j|}{h} \leq \lambda, \quad (5)$$

where the multiplier $\lambda=2$, D is the number of spatial dimensions and N is the normalisation constant equal to 1, $2/\pi$ and $5/(4\pi)$ in one, two and three dimensions, respectively, Fig. 1.

An application of the relations (1) and (2) to the Euler equations describing an isothermal flow of inviscid fluid with absence of external body forces yields the symmetric form of the SPH equations for conservation of mass and momentum in the material frame

$$\frac{d\rho_i}{dt} = \sum_j m_j (\mathbf{v}_i - \mathbf{v}_j) \cdot \nabla_i W_{ij}, \quad (6)$$

$$\frac{d\mathbf{v}_i}{dt} = -\sum_j m_j \left(\frac{p_i}{\rho_i^2} + \frac{p_j}{\rho_j^2} \right) \nabla_i W_{ij} + \frac{\mathbf{F}_i}{\rho_i}, \quad (7)$$

where ρ is the density, \mathbf{v} is the velocity vector, p is the pressure, \mathbf{F} is the body force and W_{ij} is the smoothing function $W(|\mathbf{r}_i - \mathbf{r}_j|, h)$. Within the presented SPH model, the incompressible flow is approximated using a slightly compressible fluid, Monaghan (1994), with equation of state

$$p_i = {}^0p_i + K \left[\left(\frac{\rho_i}{{}^0\rho_i} \right)^\gamma - 1 \right], \quad K = {}^0\rho \frac{{}^0c^2}{\gamma}, \quad (8)$$

where K is the bulk modulus, 0c is the initially defined sound speed and γ is a constant parameter. A constant 0p , ${}^0\rho$ respectively, indicates the initial pressure, the initial density respectively. When the applied sound speed is at least ten times higher than the maximum bulk velocity (Mach number is less or equal 0.1), the fluid is assumed to be quasi-incompressible. The parameter $\gamma=7$ is usually considered.

When a viscous fluid is being modelled, the viscous term has to be included within the Euler equations. That yields the system of the Navier-Stokes equations where the physical viscosity term implies the second order derivatives of the velocity vector. Morris et al. (1997) introduced an SPH model approximating the dissipation term in the Navier-Stokes equation in the following form

$$\left[\left(\frac{1}{\rho} \nabla \cdot \mu \nabla \right) \mathbf{v} \right]_i \approx \sum_j \frac{m_j}{\rho_i \rho_j} \frac{\mu_i + \mu_j}{|\mathbf{r}_i - \mathbf{r}_j|^2 + \eta^2} [(\mathbf{r}_i - \mathbf{r}_j) \cdot \nabla_i W_{ij}] (\mathbf{v}_i - \mathbf{v}_j) \quad (9)$$

where μ is the dynamic viscosity. The relation (9) is a hybrid expression combining a standard SPH and a finite difference approximation of the first derivative.

In the regions of sharp discontinuities, the numerical solution of the problem may be corrupted by numerical oscillations. In order to smooth the numerical oscillations and stabilise the computation when shocks occur, the von Neumann-Richtmeyer like SPH artificial viscosity term is introduced within the pressure term in the equation (7), Monaghan & Gingold (1983),

$$\Pi_{ij} = \begin{cases} \frac{1}{2} \beta \frac{(h_i + h_j)^2}{\rho_i + \rho_j} \left(\frac{(\mathbf{v}_i - \mathbf{v}_j)(\mathbf{r}_i - \mathbf{r}_j)}{|\mathbf{r}_i - \mathbf{r}_j|^2 + \eta^2} \right)^2, & (\mathbf{v}_i - \mathbf{v}_j) \cdot (\mathbf{r}_i - \mathbf{r}_j) < 0, \\ 0, & (\mathbf{v}_i - \mathbf{v}_j) \cdot (\mathbf{r}_i - \mathbf{r}_j) \geq 0, \end{cases} \quad (10)$$

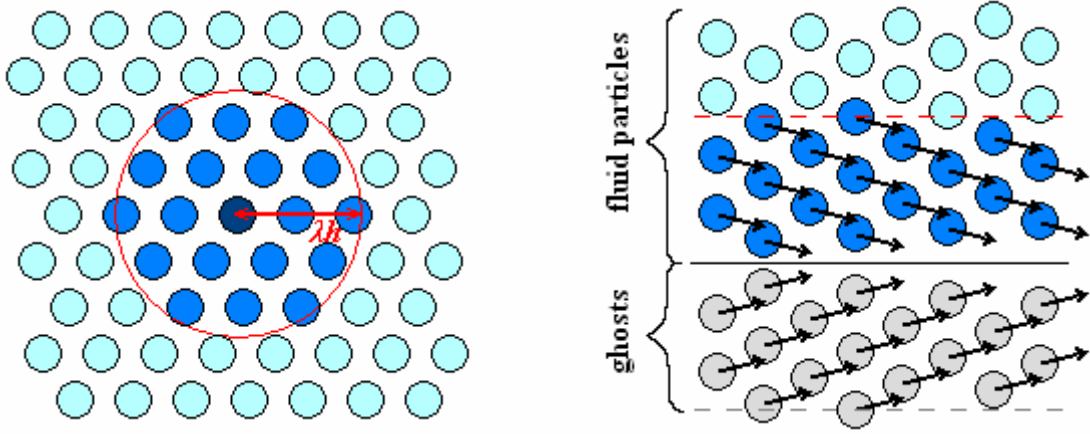


Fig. 2. The distribution of particle's neighbours in a smoothing function support domain (left), reflecting the fluid particles and their velocities across the boundary line (right).

where h is the smoothing length, β is a constant artificial viscosity parameters and η is an anti-crossing parameter $\eta=0.01H^2$, where H is an average smoothing length $H=0.5(h_i+h_j)$. The artificial viscosity term (10) is positive when particles are approaching each other and null otherwise. That helps to prevent unphysical particle interpenetration. The resulting set of the SPH governing equations becomes

$$\frac{d\rho_i}{dt} = \sum_j m_j (\mathbf{v}_i - \mathbf{v}_j) \cdot \nabla_i W_{ij}, \quad (11)$$

$$\frac{d\mathbf{v}_i}{dt} = -\sum_j m_j \left(\frac{p_i}{\rho_i^2} + \frac{p_j}{\rho_j^2} + \Pi_{ij} \right) \nabla_i W_{ij} + \sum_j \frac{m_j}{\rho_i \rho_j} \frac{\mu_i + \mu_j}{|\mathbf{r}_i - \mathbf{r}_j|^2 + \eta^2} [(\mathbf{r}_i - \mathbf{r}_j) \cdot \nabla_i W_{ij}] (\mathbf{v}_i - \mathbf{v}_j) + \frac{\mathbf{F}_i}{\rho_i} \quad (12)$$

When a spatial resolution of the particles may vary during the calculation, the smoothing length value may be updated in order to keep the constant number of neighbouring particles, Fig. 2 (left). In order to do so, the following relation is considered

$$\frac{dh_i}{dt} = \frac{h_i}{D} \sum_j \frac{m_j}{\rho_j} (\mathbf{v}_i - \mathbf{v}_j) \cdot \nabla_i W_{ij}. \quad (13)$$

Solid boundaries of the fluid can be modelled by ghost particles, Fig. 2 (right), which symmetrically reflect the fluid particles across the boundary surface, Libersky et al. (1993), Colagrossi & Landrini (2003). The width of the reflected boundary region is defined by the smoothing function support λh . At every timestep, positions and all variables assigned to the ghost particles are updated according to the positions and actual properties of the fluid particles close to the boundary. The ghost particles have assigned the same density and pressure as the corresponding fluid particles. In order to model the free-slip boundary conditions, the velocity vector of the ghost particle is derived from the fluid particle's velocity vector so that it has the same value in tangential direction to the boundary and the opposite value in the direction of the boundary normal.

The time integration of SPH equations is performed using a predictor-corrector scheme and the timestep is determined according to the Courant-Friedrich-Lewy condition, Morris et al. (1997).

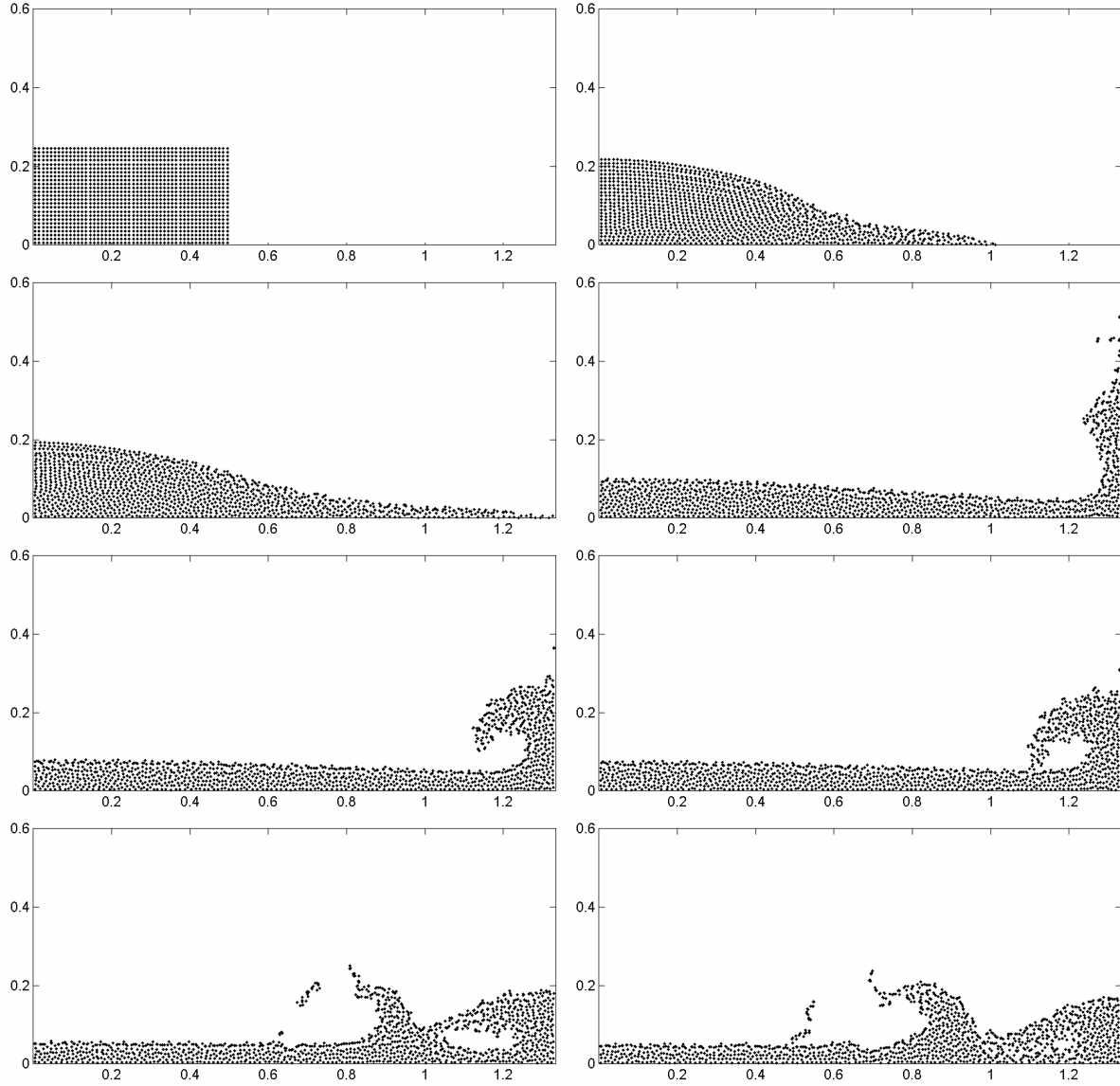


Fig. 3. The bursting dam simulation, distribution of fluid particles at time 0 s, 0.27 s, 0.38 s, 0.76 s, 0.91 s, 0.94 s, 1.175 s and 1.265 s, respectively.

3. Results and Discussion

The implemented SPH code is applied to various gravity current flows. The presented numerical simulations are focused on the problems involving the free surface boundaries, the fluid to rigid wall and fluid to fluid interaction. All computations are performed for quasi-incompressible viscous fluids in a two dimensional space while the boundary walls are supposed to be absolutely rigid and smooth-surfaced.

The first presented problem concerns about the evolution of the fluid flow after a sudden removal of a vertical dam, Fig. 3. The height of the fluid contained within the dam is 0.25 m and its width is 0.5 m. The fluid density is $1000 \text{ kg}\cdot\text{m}^{-3}$ and its viscosity is $8.9\times 10^{-4} \text{ Pa}\cdot\text{s}$. The gravitational acceleration $9.81 \text{ m}\cdot\text{s}^{-2}$ is applied. When the dam is removed, the fluid flow is generated by the gravitational force along the initially dry bottom-deck. At a distance of 0.83 m from the dam, the fluid impacts the vertical wall. The flow runs up, turns backwards

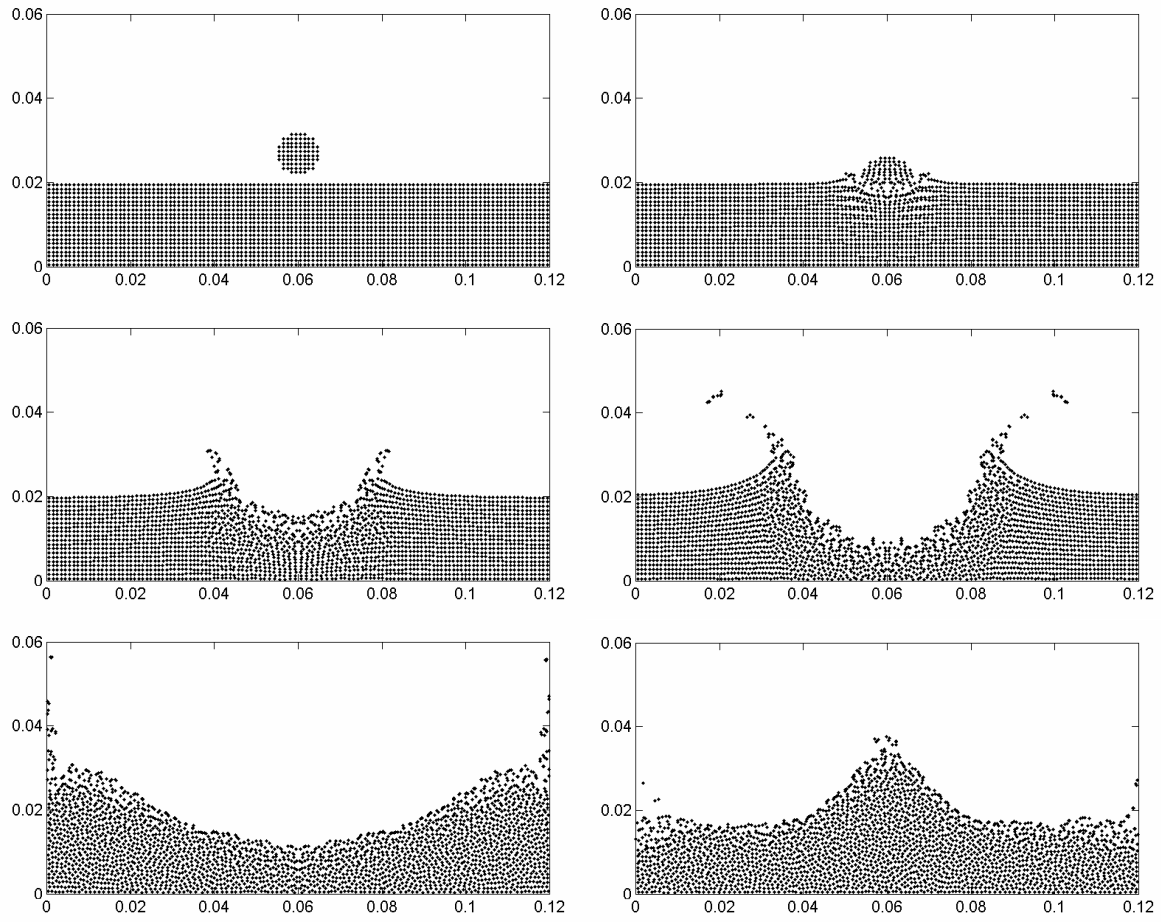


Fig. 4. Simulation of the fluid drop falling into the pool, distribution of fluid particles at time 0 s, 0.003 s, 0.013 s, 0.033 s, 0.114 s and 0.205 s, respectively.

and a fluid wave falls onto the underlying fluid. The simulation is performed using 1250 fluid particles which are distributed regularly with an initial inter-particle distance of 0.01 m. The initial smoothing length is chosen 1.33 times the initial distance between particles, the initial sound speed is set to $24.4 \text{ m}\cdot\text{s}^{-1}$ and the value of the artificial viscosity parameter is 1. The non-zero artificial viscosity parameter prevents the particle interpenetration, thus it helps to keep particles ordered. That is significant especially during the fluid impact on the vertical wall and during the overturning of the fluid flow which results in fluid to fluid impact. Eventhough the quasi-incompressible model is used, the resulting volume variations are less then 0.3 %. The wave front propagation and the corresponding height of the fluid column during the downstream motion agrees well with the data published in Monaghan (1994) and Liu & Liu (2003). The character of the overturned flow including the wave breaking corresponds to the results published in Colagrossi & Landrini (2003).

The second example presents the problem of the circular fluid drop falling into the pool of fluid with the same properties, Fig. 4. The pool is 0.12 m wide, the initial fluid depth is 0.02 m and the fluid drop diameter is 0.01 m. The gravitational acceleration is $9.81 \text{ m}\cdot\text{s}^{-2}$. The drop impacts the fluid free surface at the velocity of $2 \text{ m}\cdot\text{s}^{-1}$. The fluid in pool is initially at rest. After the impact, a splash is formed and the waves propagate along the pool. The simulation is performed for 2480 regularly distributed fluid particles. The initial smoothing

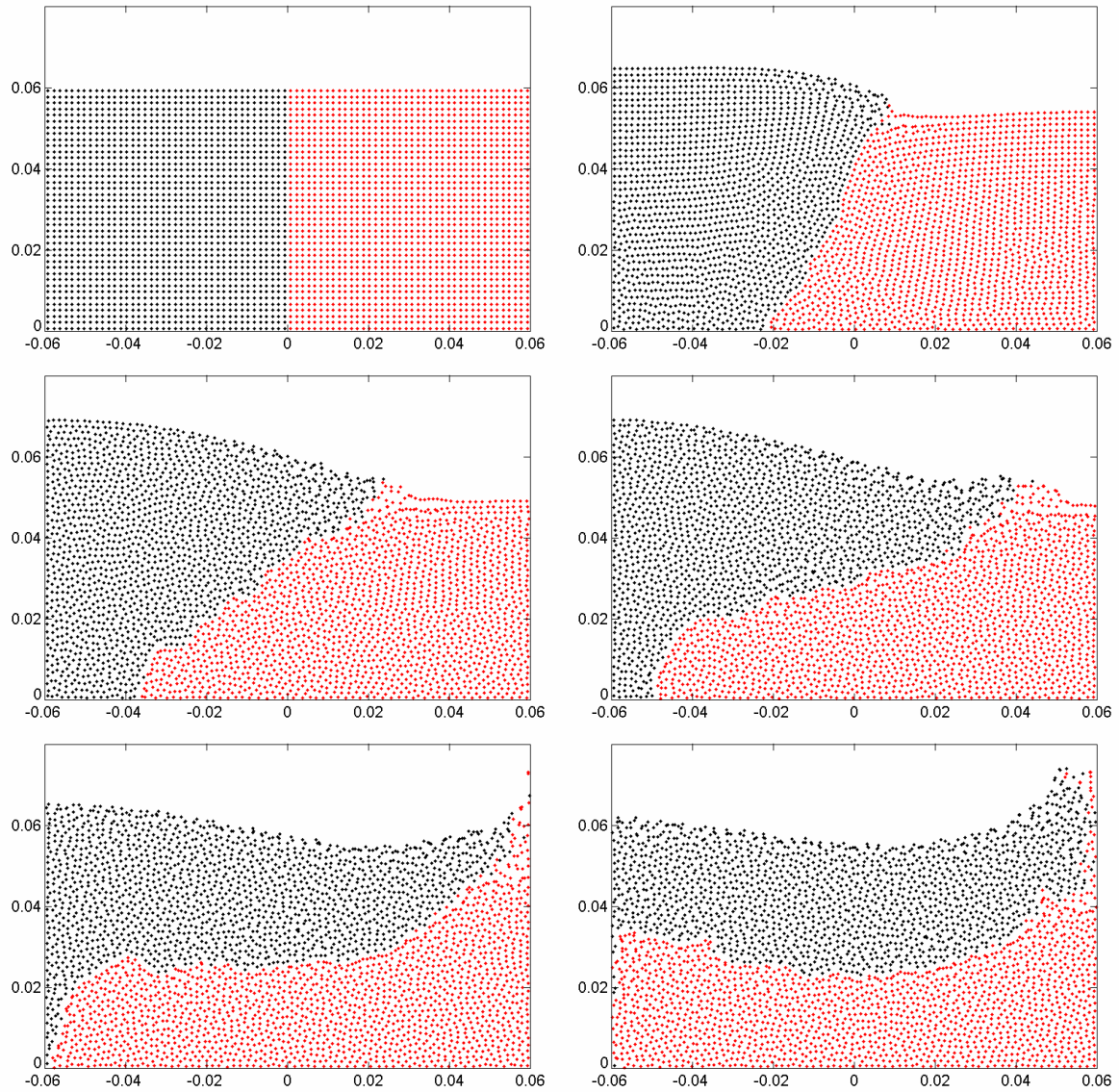


Fig. 5. The gravity current flow of two immiscible fluids with different densities, distribution of fluid particles at time 0 s, 0.11 s, 0.17 s, 0.23 s, 0.29 s and 0.35 s, respectively.

length is 1.33 times the initial distance between particles, which is 0.001 m. The density and the viscosity of the fluid, the sound speed value and the artificial viscosity parameter are kept the same as in the previous example. The quasi-incompressible fluid model results in overall volume variations of about 0.2 %. The results show quite reasonable behaviour of the fluid flow, which might be expected for such a kind of impact when the fluid drop impacts the shallow fluid pool. Unfortunately no precise experimental data are available to the authors at the moment. When compared to the results published by Cueto-Felgueroso et al. (2005), a qualitatively good agreement is observed.

The third problem presents the interaction of two immiscible fluids with different densities. The fluids are in a rectangular tank which is divided by a vertical dam into two parts of the same size. The width of the entire tank is 0.12 m and the initial fluid depth is 0.06 m. Both fluids are at rest initially. The density of the fluid in the left and the right part is $1000 \text{ kg}\cdot\text{m}^{-3}$

and $1500 \text{ kg}\cdot\text{m}^{-3}$, respectively. Both fluids have the same viscosity of $8.9\times 10^{-4} \text{ Pa}\cdot\text{s}$. When the dam is removed, the thicker fluid starts to move under the thinner fluid. Thus a wave of the thinner fluid move in an opposite direction. The flow of both fluids is driven according to the gravitational acceleration $9.81 \text{ m}\cdot\text{s}^{-2}$. There are 3200 regularly distributed fluid particles involved in the calculation. The initial inter-particle distance is 0.001 m and the initial smoothing length is 1.33 times higher. As no excessive shocks are expected within the simulation, there is no need to introduce an additional numerical stabilisation into the model. Thus the artificial viscosity parameter is kept zero. The speed of sound is set to $24.4 \text{ m}\cdot\text{s}^{-1}$ which results in fluid volume variations less than 0.2 %. The character of the flow and the propagation of the fluid waves agrees well with the data published in Cueto-Felgueroso et al. (2005). In the end of the simulation, the thicker fluid settles down below the thinner fluid.

4. Conclusion

The implemented SPH code involving the quasi-incompressible fluid model, the artificial viscosity term, the variable smoothing length and the free-slip ghost boundary conditions is capable of simulating free surface flows including fluid to rigid wall and fluid to fluid interactions. The computed results give a satisfactory agreement with the data published in the literature.

5. Acknowledgement

This work is supported by the research project MSM 4977751303 of the Ministry of Education, Youth and Sports of the Czech Republic.

6. References

- Colagrossi, A., Landrini, M. (2003) Numerical simulation of interfacial flows by smoothed particle hydrodynamics. *Journal of Computational Physics*, 191, pp. 448-475.
- Cueto-Felgueroso, L., Colominas, I., Navarrina, F., Casteleiro, M. (2005) Numerical simulation of free surface flows by Lagrangian particle methods. *Fluid Structure Interaction and Moving Boundary Problems*, WIT Press, Southampton, pp. 491-500.
- Gingold, R.A., Monaghan, J.J. (1977) Smoothed Particle Hydrodynamics: theory and application to non-spherical stars. *Monthly Notices of the Royal Astronomical Society*, 181, pp. 375-389.
- Libersky, L.D., Petschek, A.G., Carney, T.C., Hipp, J.R., Allahdadi, F.A. (1993) High strain Lagrangian hydrodynamics. *Journal of Computational Physics*, 109, pp. 67-75.
- Liu, G.R., Liu, M.B. (2003) *Smoothed Particle Hydrodynamics*. World Scientific Publishing, Singapore.
- Lucy, L. (1977) A numerical approach to the testing of the fission hypothesis. *Astronomical Journal*, 82, pp. 1013-1020.
- Monaghan, J.J., Gingold, R.A. (1983) Shock simulation by the particle method SPH. *Journal of Computational Physics*, 52, pp. 374-389.

- Monaghan, J.J. (1992) Smoothed Particle Hydrodynamics. *Annual Review of Astronomy and Astrophysics*, 30, pp. 543-574.
- Monaghan, J.J. (1994) Simulating free surface flows with SPH. *Journal of Computational Physics*, 110, pp. 399-406.
- Monaghan, J.J., Kocharyan, A. (1995) SPH simulation of multi-phase flow. *Computer Physics Communications*, 87, pp. 225-235.
- Morris, J.P., Fox, P.J., Zhu, Y. (1997) Modeling low Reynolds number incompressible flows using SPH. *Journal of Computational Physics*, 136, pp. 214-226.
- Vignjevic, R. (2004) Review of development of the Smooth Particle Hydrodynamics (SPH) method. *Proc. of 6th Conference on Dynamics and Control of Systems and Structures in Space*, Cranfield University, pp. 23-44.